



# New Intelligent Power Adjustment of the Wind Energy Conversion System Extended Virtual Flux based Direct Power Control Using New Fuzzy-PI Controller

Hamed Kamel Eddine Zine<sup>1,\*</sup>, Razik. Dib<sup>2</sup> and Khoudir Abed<sup>3</sup>

<sup>1,2,3</sup> Department of electrical engineering, Faculty of Engineering Sciences Mentouri University, Road Ain El Bey, Constantine, Algeria.

\*Corresponding author. Email address: kamel-eddine.zine-hamed@lec-umc.org

## Abstract

In this paper, a new DPC-VF power adjustment is proposed for wind energy conversion systems (WECS) based Doubly Fed Induction Generator (DFIG) drive system, feed through an ameliorate voltage rectifier. The efficiency of the proposed DPC-Virtual flux in handling nonlinear systems such as a Doubly Fed Induction Generator has been effectively demonstrated by comparing DPC-VF estimation using new Fuzzy-PI controller with Indirect Field oriented control under varying operating conditions like step change in stator active power reference and stator reactive power reference.

**Keywords:** wind energy conversion systems, Doubly Fed Induction Generator, IFOC, DPC-VF, Fuzzy-PI Controller.

## 1. Introduction

Global energy consumption continues to increase, the large part of this consumable energy comes from fossil fuels (oil, natural gas, coal, etc.), the massive use of which can lead to the depletion of these reserves and really threatens the environment.

The wind energy is clean and renewable energy, unlike conventional energy which presents the constraints of distance from the electricity network and the constraints of fuel transport, as well as the periodic maintenance of the installations.

PWM rectifiers are inverters that operate in the opposite direction to their usual direction of energy transfer. When a PWM rectifier is placed between the AC network and a DC receiver, it is the network that imposes the frequency of the voltages and, consequently, the currents that are drawn from it. The frequency of the reference waves which are used for the PWM cutting is therefore imposed. But, by acting on the amplitude and the setting of the reference

waves with respect to the network voltages, we can adjust the value of the rectified voltage and put the fundamental of the current absorbed by each phase in phase with the voltage of this one, that is, to operate at  $\cos(\varphi)$  equal to unity.

On the other hand, by using a sufficiently high modulation frequency, we can push the harmonics of the absorbed currents towards high frequencies and facilitate their filtering [1].

The vector control of the double fed asynchronous generator is a more attractive solution for high performance applications in variable speed and power generation systems, where the principle and different methods of vector control as well as the control of the connection to the electrical network [2].

VF-DPC control is another type of high performance control strategy for PWM converters based on the proposed power theory [3]. The basic idea of this control is to choose the best switching state of the power switches through a switching table with hysteresis comparisons to maintain a purely



sinusoidal current and also achieve a unity power factor.

The DFIG, thanks to its dual power supply, offers several possibilities for reconfiguring the operating mode. Thus, it has good performance, either in over speed operation or in low speed operation. The converter -machine-control unit now allows flexibility, precision and reliability to be combined with today's energy saving requirements. The joint progress of power electronics and digital electronics has made it possible to develop several control approaches to control the operation of electric machines in real time.

The resolution of the problems of pure integration, more researchers focus on replacing the pure integrator by using Indirect Field Oriented Control, 'IFOC', consists in adjusting the flux by a component of the current and the torque by the other component. For this purpose, it is necessary to choose a d-q reference frame rotating synchronously with the rotor flux space vector, in order to achieve decoupling control between the flux and the produced torque. This technique allows to obtain a dynamical model similar to the DC machine [13-15], however, the problem of flux, control structure, System stability (Active Power Ps), PWM, amplitude and phase deviation is caused.

In order to overcome the influence of integral initial value and cumulative deviation of pure integrator, and avoid the amplitude and phase deviation caused by IFOC, this paper proposes a new method for Virtual Flux estimation that is inherently capable of handling these problems, as a result a

stable and smooth virtual flux estimated and DC link voltage and sector detection with precision and more System stability (Active Power Ps). The suggested method is based on utilizing new Fuzzy-PI Controller [16-17].

This paper is divided into seven sections. In Section 1, the introduction is presented. In Section 2, the Field oriented control structure, modeling of the turbine, modeling of multiplier, DFIG modeling are described. The design of Fuzzy-PI Controller has been discussed in Section 3. In Section 4, the description of Virtual flux based direct power control 'VF-DPC', Hysteresis regulators, Switching table, Measurement instantaneous Powers by Flux Estimation are presented. Simulation results studies are presented and discussed in Section 5. Comparison to the state of the art is summarized in section 6. The conclusions are provided in Section 7.

## 2. Field Oriented Control Structure

A block diagram for an IFOC can be seen in Figure 1. This design uses a more robust structure known as Indirect Field Oriented Control [5].

In this drive system, the indirect flux oriented control of DFIG using the Fuzzy-PI Controller. The diagram contains the calculation blocks for the desired rotor currents and voltages, the PARK transformation blocks, a PWM inverter on the rotor side, and the model of the DFIG in the PARK frame-dq.

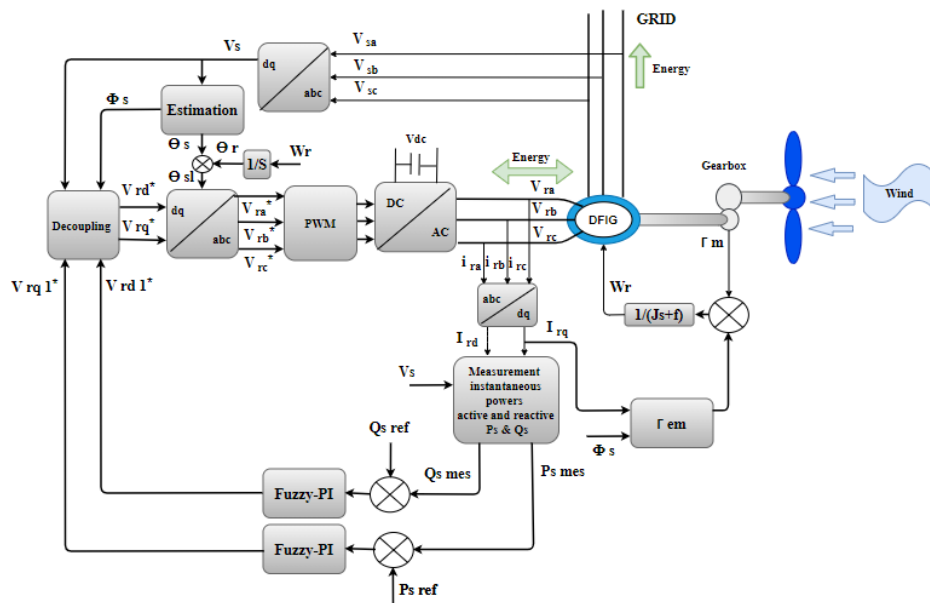


Figure 1. Field oriented controller block diagram

## 2.1. The modeling of the turbine

The modeling of the turbine consists in expressing the extractable power as a function of the wind speed and the operating conditions; this makes it possible to know the wind torque applied to the wind turbine. This modeling is based on bibliographic cross-checking or additional information from brochures from different manufacturers.

$$P_{aer} = \frac{1}{2} C_p(\lambda, \beta) \rho S V_v^3 = \frac{1}{2} \rho \pi R_T^2 V_v^3 \quad (1)$$

With:

$$\lambda = \frac{\Omega_T R_T}{V_v} \quad (2)$$

$\lambda$ : The speed ratio (rad), defined as the ratio between the linear speed of the blades  $\Omega_T$  and the wind speed  $V_v$ .  $\beta$ : The orientation angle of the blades.  $\Omega_T$ : Turbine rotation speed.  $R_T$ : The length (radius) of the blade.  $V_v$ : The wind speed.  $\rho$ : is the density of the air (1.22 kg/m<sup>3</sup> at atmospheric pressure at 15°C). The Betz limit is that the power coefficient  $C_p(\lambda, \beta)$  does not exceed the value  $\frac{16}{27} = 0.59$  [4].

## 2.2. Modeling of the multiplier

The turbine speed must be adjusted to the generator speed (DFIG). For this we grant a multiplier between the turbine and the DFIG, the latter is mathematically modeled by the following equations:

$$C_g = \frac{C_T}{G} \quad (3) \quad \Omega_T = \frac{\Omega_{mec}}{G} \quad (4)$$

The mechanical equation:

$$\frac{C_T}{G} - C_g = \left( \frac{J_T}{G^2} + J_g \right) \frac{d\Omega_{mec}}{dt} + \left( \frac{f_T}{G} + f_g \right) \Omega_{mec} \quad (5)$$

$$\frac{J_T}{G^2} + J_g = J \quad (6)$$

$$\frac{f_T}{G} + f_g = f \quad (7)$$

So the mechanical equation will be like:

$$C_{mec} = J \frac{d\Omega_{mec}}{dt} \quad (8)$$

$$C_{mec} = C_g - C_{em} - C_{vis} \quad (9)$$

$$C_{vis} = f \Omega_{mec} \quad (10)$$

$C_T, C_g, C_{vis}$ : The wind couple, the electromagnetic couple and the viscous couple.  $J_T, J_g$ : The inertia of the turbine and that of the generator.  $f_T, f_g$ : The coefficient of viscous friction of the turbine and that of the generator.  $G$ : The ratio of the speed multiplier.  $\Omega_{mec}$ : The generator rotation speed (fast axis).

## 2.3. DFIG modeling

So, the DFIG mathematical model is written in Park's frame of reference linked to the field turn as follows [4]:

The equations of tensions:

$$\begin{cases} V_{ds} = R_s \cdot I_{ds} + \frac{d\phi_{ds}}{dt} - \omega_s \cdot \phi_{qs} \\ V_{qs} = R_s \cdot I_{qs} + \frac{d\phi_{qs}}{dt} + \omega_s \cdot \phi_{ds} \\ V_{dr} = R_r \cdot I_{dr} + \frac{d\phi_{dr}}{dt} - (\omega_s - \omega) \cdot \phi_{qr} \\ V_{qr} = R_r \cdot I_{qr} + \frac{d\phi_{qr}}{dt} + (\omega_s - \omega) \cdot \phi_{dr} \\ \int \frac{d\Omega_r}{dt} = C_{em} - C_r - f_r \cdot \Omega_r \end{cases} \quad (11)$$

The equations of the Fields:

$$\begin{cases} \phi_{ds} = L_s \cdot I_{ds} + M \cdot I_{dr} \\ \phi_{qs} = L_s \cdot I_{qs} + M \cdot I_{qr} \\ \phi_{dr} = L_r \cdot I_{dr} + M \cdot I_{ds} \\ \phi_{qr} = L_r \cdot I_{qr} + M \cdot I_{qs} \end{cases} \quad (12)$$

$$C_{em} = \frac{M}{L_r} p (\phi_{dr} I_{qs} - \phi_{qr} I_{ds}) \quad (13)$$

The electromagnetic couple becomes:

$$C_{em} = \frac{3}{2} \frac{M}{L_s} p (\phi_{qs} I_{rd} - \phi_{sd} I_{rq}) \quad (14)$$

The stator and rotor active and reactive powers are expressed by:

$$\begin{cases} P_s = \frac{3}{2} (V_{sd} I_{sd} + V_{sq} I_{sq}) \\ Q_s = \frac{3}{2} (V_{sq} I_{sd} - V_{sd} I_{sq}) \\ P_r = \frac{3}{2} (V_{rd} I_{rd} + V_{rq} I_{rq}) \\ Q_r = \frac{3}{2} (V_{rq} I_{rd} - V_{rd} I_{rq}) \end{cases} \quad (15)$$

$R_s, R_r$ : stator and rotor resistances.

$L_s, L_r, M$ : respectively stator, rotor, mutual inductances.

$I_{ds}, I_{qs}, I_{dr}, I_{qr}$ : respectively stator and rotor currents in the dq frame.

$P_s, Q_s, P_r, Q_r$ : stator and rotor active and reactive powers.

$V_{ds}, V_{qs}, V_{dr}, V_{qr}$ : stator and rotor voltage components in the dq frame.

$\omega_s$ : speed of stator magnetic field.

$\omega_r = \omega_s - \omega$ : angular speed of rotor.

In what follows we will assume that the d axis of Park's coordinate system is oriented along with the stator flux. This choice is not at random but it is justified by the fact that the machine is often coupled



to a powerful network of constant voltage and frequency, which causes a constant flux to the stator of the machine [6][7].

Figure 2. illustrates stator field oriented control technique.

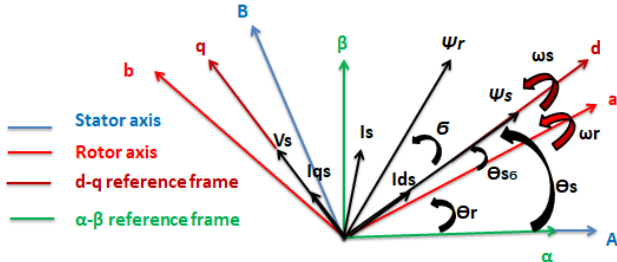


Figure 2. Stator field oriented control technique.

We set ( $\phi_{ds} = \phi_s$  and  $\phi_{qs} = 0$ ), we find :

$$\begin{cases} \phi_{sd} = L_s \cdot I_{sd} + M I_{rd} = \phi_s \\ \phi_{sq} = L_s \cdot I_{sq} + M I_{rq} = 0 \\ \phi_{rd} = L_r \cdot I_{rd} + M I_{sd} \\ \phi_{rq} = L_r \cdot I_{rq} + M I_{sq} \end{cases} \quad (16)$$

From the stator field equation and according to the field orientation condition, the stator currents are expressed by:

$$\begin{cases} I_{sd} = \frac{(\phi_{sd} - M I_{rd})}{L_s} \\ I_{sq} = \frac{\phi_{sq} - M I_{rq}}{L_s} \end{cases} \quad (17)$$

By replacing the two components of the stator current in the electromagnetic torque equation (14), the following expression is obtained:

$$C_{em} = \frac{-PM}{L_s} \phi_s I_{rq} \quad (18)$$

According to this equation and for  $\frac{-PM}{L_s} \phi_s$  constant, the electromagnetic torque can be controlled by the current  $I_{rq}$ . Then, the torque  $C_{em}$  of the DFIG can take a shape similar to that of the DC machine.

If the resistance of the stator  $R_s$  is neglected the stator voltages  $V_{sd} V_{sq}$  are:

$$\begin{cases} V_{sd} = \frac{d\phi_{sd}}{dt} = 0 \\ V_{sq} = \omega_s \phi_{sd} = V_s \end{cases} \quad (19)$$

Thus in this benchmark, taking into account the hypotheses made, the active and reactive powers then become:

$$\begin{cases} P_s = V_{sd} \cdot I_{sd} + V_{sq} \cdot I_{sq} \\ Q_s = V_{sq} \cdot I_{sd} - V_{sd} \cdot I_{sq} \end{cases} \quad (20)$$

According to the conditions of the stator field orientation can write the active and reactive power relationship in the following form:

$$\begin{cases} P_s = V_{sq} \cdot I_{sq} \\ Q_s = V_{sd} \cdot I_{sd} \end{cases} \quad (21)$$

By replacing the stator currents with their values of

equation (17) and the value of  $\phi_s$  of equation (16) in equation (21), we obtain the following expressions for the active and reactive powers.

$$\begin{cases} P_s = -V_s \cdot \frac{M}{L_s} I_{rq} \\ Q_s = \frac{V_s \cdot \phi_s}{L_s} - \frac{V_s \cdot M}{L_s} I_{rd} \end{cases} \quad (22)$$

### 3. Design Of Fuzzy-PI Controller

The Fuzzy logic is applied to optimize the PI controller gains which are designed to optimize the step response of the system [8][9].

The purpose of this design is to synthesize a controller without the exact knowledge of a model, numerically simple, and simulated on Matlab/Simulink allowing good performance in terms of overshoot, fast and accuracy under the power Active, Reactive and voltage rectifier variations.

The Fuzzy Logic Toolbox based controller architecture is shown in Figure 3.

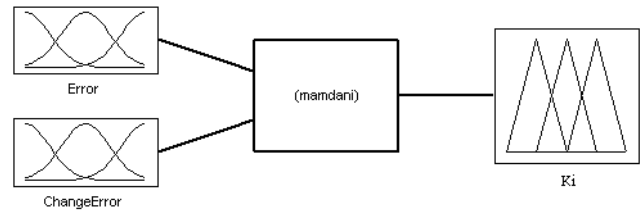


Figure 3. Fuzzy controller architecture

The fuzzy logic controller employs Active and Reactive Powers and DC Link Voltage error and its rate of change as inputs, the  $K_i$  of the PI controller is output.

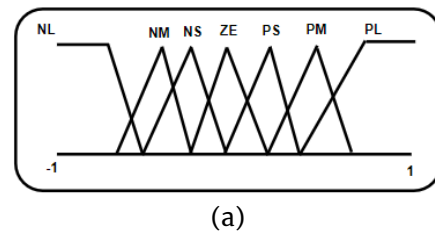
$$e(k) = V_{dc}^* - \hat{V}_{dc} \quad (23)$$

$$e(k) = Q_s^* - \hat{Q}_s \quad (24)$$

$$e(k) = P_s^* - \hat{P}_s \quad (25)$$

$$\Delta e(k) = e(k) - e(k-1) \quad (26)$$

And it uses the following linguistic labels: {NL (Negative Large), NM (Negative Medium), NS (Negative Short), ZE (Zero), PS (Positive Short), PM (Positive Medium), PL (Positive Large)}. Each fuzzy label has an associated membership function. The membership functions as shown in Figure 4.



(a)

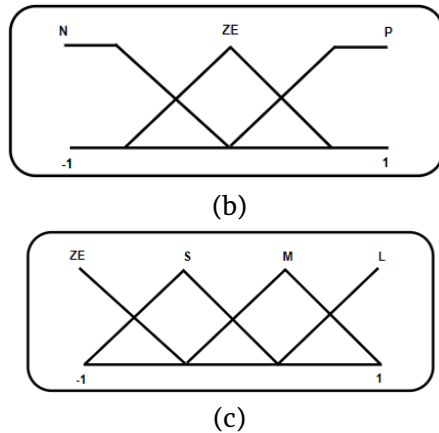


Figure 4. Membership function of input, output variables, (a) Error, (b) Change of Error, (c) Ki.

The input membership functions Error E, ΔE change Error are expressed by triangle and Trapezoidal curve, and The output membership function Ki is expressed by triangle, as shown in Figure 4. They are defined in the interval [-1, 1].

The control rules are represented as a set of then rules. The seven fuzzy rules of the proposed controller for power or DC voltage control of doubly fed induction generator are selected relative to proximity and distance, negative and positive from zero for more System stability and precision, and are presented in Table 1. And formulated as follows:

If e (k) is NL and Δe (k) is N then Ki (k) is ZE.

Table 1. Control rule base

E	NL	NM	NS	ZE	PS	PM	PL
CE							
ZE	ZE	S	M	L	M	S	ZE
P	ZE	M	L	L	L	M	ZE
N	ZE	S	M	L	M	S	ZE

The present design uses Mamdani's Max-Min algorithm for inference mechanism.

De-fuzzification process: uses centre gravity of area technique to convert fuzzy values to crisp values. This method provides easy computation and accurate results. The output of this system is the overall performance of Active and Reactive Powers or DC Link Voltage, Faculty's overall performance = Negative Large/Negative Medium/Negative Short/Zero/Positive Short/Positive Medium/Positive Large [18]. The Fuzzy PI control system structure is given in this paper, shown as Figure 5.

$$\Delta\mu_0 = \frac{\sum_{j=0}^n C^0(\Delta\mu_j) \cdot \Delta\mu_j}{\sum_{j=0}^n C^0(\Delta\mu_j)} \quad (27)$$

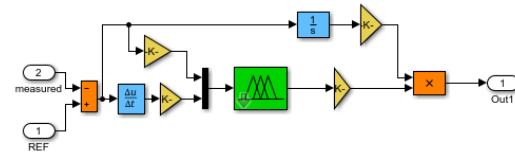


Figure 5. Simulink model of fuzzy controller for DFIG.

#### 4. Virtual flux based direct power control 'VF-DPC'

Direct power control (DPC) is based on the concept of direct torque control applied to electric machines. The aim is to directly control the active and reactive power in a PWM rectifier. The errors between the reference values of the instantaneous active and reactive power and their measurements are introduced into two hysteresis comparators which determine the switching state of the semiconductors, with the help of a switching board and the value of the mains where is the generator voltage [10].

##### 4.1. Hysteresis regulators

The active and reactive power controlled by two regulators hysteresis, the measured value of the powers being estimated from relationship [11]:

$$\begin{cases} P_s = \frac{3}{2}(V_{s\alpha}i_{s\alpha} + V_{s\beta}i_{s\beta}) \\ Q_s = \frac{3}{2}(V_{s\alpha}i_{s\alpha} - V_{s\beta}i_{s\beta}) \end{cases} \quad (28)$$

$$\begin{cases} P_{s \text{ error}} = P_s^* - P_s \\ Q_{s \text{ error}} = Q_s^* - Q_s \end{cases} \quad (29)$$

Two three-level hysteresis regulators are used to generate the respective active and reactive power states Sp and Sq as Figure 6. Shows.

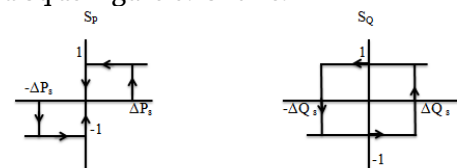


Figure 6. Active and Reactive Power hysteresis regulators.

##### 4.2. Switching table

Switching table presented in this part which uses a relatively simple technique and divides the plane into six sectors. The references of active and reactive powers values are compared with the estimated ones respectively in hysteresis controllers, with Sp and Sq

are the outputs signal of active and reactive powers controllers respectively. We elaborated the switching table of the control structure; according to the outputs of the controllers' Sp, Sq and the rotor flux position  $\delta$ . The digitized error signal Sp and Sq and the rotor flux sector are input to the switching table in which every switching state Sa, Sb, and Sc of the 2L-VSI is stored as shown in Table 2.

Table 2. Switching table of rotor voltage vector in DPC method

uQs	uPs	Secteur					
		1	2	3	4	5	6
1	1	V3	V4	V5	V6	V1	V2
	0	V0	V7	V0	V7	V0	V7
	-1	V5	V6	V1	V2	V3	V4
-1	1	V2	V3	V4	V5	V6	V1
	0	V7	V0	V7	V0	V7	V0
	-1	V6	V1	V2	V3	V4	V5

To choice the ideal rotor voltage vector, we must know the relative position of the stator flux within sixtants Figure 7. (a) .A three-phase inverter can create eight different combination as follows: V0 (0 0 0), V1 (1 0 0), V2 (1 1 0), V3 (0 1 0), V4 (0 1 1), V5 (0 0 1), V6 (1 0 1), V7 (1 1 1).

The eight combinations produce eight voltage vectors that can be applied to the rotor of the DFIG terminals. There are six active vectors and two zero vectors. The spatial positions (in the plan  $\alpha\beta$ ) voltages of active channels are shown in Figure 7

Figure 7. (b) demonstrates how the switching voltage vectors after the rotor flux vector. Application switching vector V3 during a Sampling period Ts, modifies rotor flux  $\varphi_r$  (K) into  $\varphi_r$  (K+1), which in turn has the effect of increasing  $|\varphi_r|$  and angle to  $\varphi_s$ .

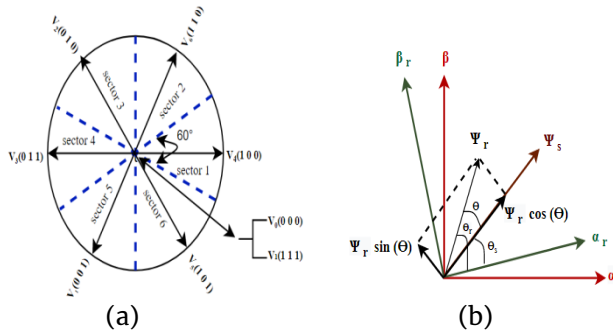


Figure 7. (a) Voltage vectors and the control of flux using voltage vectors, (b) The space vectors of stator and rotor flux different

reference frames.

### 4.3. Measurement instantaneous powers by Flux estimation

The flux, in addition to being present for synchronization, is also used for the calculation of instantaneous powers. Thus, the integration of the generator voltage generates a flux vector in the coordinates ( $\alpha\beta$ ), see equation (33). The voltage drop across the resistor has been neglected [12].

$$V = e + Ri + L \frac{di}{dt} \tag{30}$$

$$e = V - (Ri + L \frac{di}{dt}) \tag{31}$$

$$\Psi = \int e dt \tag{32}$$

$$\begin{cases} \Psi_\alpha = \int e_\alpha dt = \int (V_\alpha - L \frac{di_\alpha}{dt}) dt \\ \Psi_\beta = \int e_\beta dt = \int (V_\beta - L \frac{di_\beta}{dt}) dt \end{cases} \tag{33}$$

Where:

$\Psi$ : is the estimated flux and V is the converter voltage.

By considering the voltage of the inverter in coordinates  $\alpha\beta$ , the expression of the flux becomes the following:

$$\begin{cases} \Psi_\alpha = \int (\sqrt{\frac{2}{3}} U_{dc} (S_a - \frac{1}{2}(S_b + S_c))) dt - Li_\alpha \\ \Psi_\beta = \int (\sqrt{\frac{2}{3}} U_{dc} (S_b - S_c)) dt - Li_\beta \end{cases} \tag{34}$$

The voltage is obtained from the estimated flux:

$$\bar{e} = \frac{d\bar{\Psi}}{dt} = \frac{d\Psi}{dt} e^{j\omega t} + j \omega \Psi e^{j\omega t} = \frac{d\Psi}{dt} e^{j\omega t} + j \omega \bar{\Psi} \tag{35}$$

Where:

$\bar{\Psi}$ : is the vector of the estimated flux.

$\Psi$ : The amplitude of the estimated flux.

This method works in  $\alpha\beta$  coordinates. Thus, the instantaneous powers are calculated as follows:

$$\begin{cases} P = e_\alpha i_\alpha + e_\beta i_\beta \\ Q = e_\beta i_\alpha + e_\alpha i_\beta \end{cases} \tag{35}$$

Knowing that for almost sinusoidal and balanced voltages the derivatives of the flux amplitude are zero, the instantaneous active and reactive powers are calculated by the equation below.

$$\begin{cases} P = \omega (\Psi_\alpha i_\beta - \Psi_\beta i_\alpha) \\ Q = \omega (\Psi_\alpha i_\alpha + \Psi_\beta i_\beta) \end{cases} \tag{36}$$

Figure 8. illustrates the direct power control Fuzzy PI using virtual flux estimation .

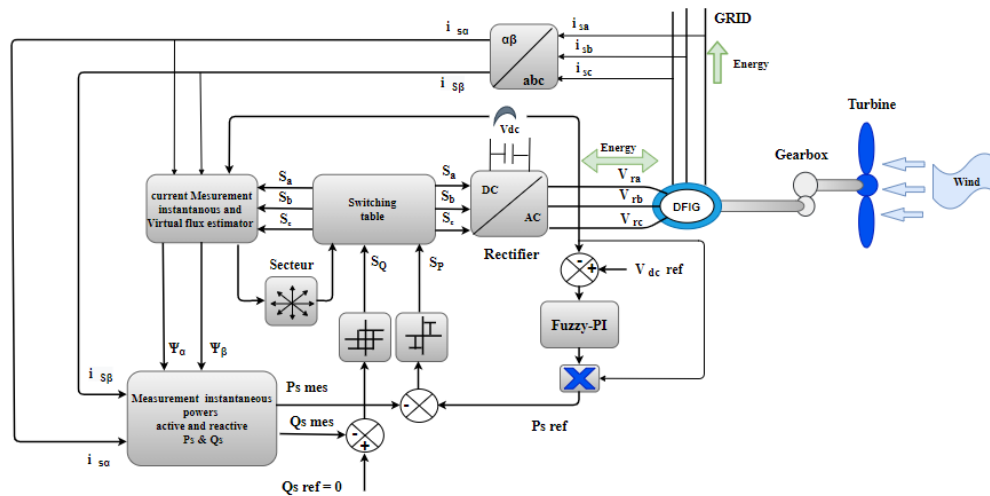


Figure 8. Block diagram of VF-DPC strategy for DFIG.

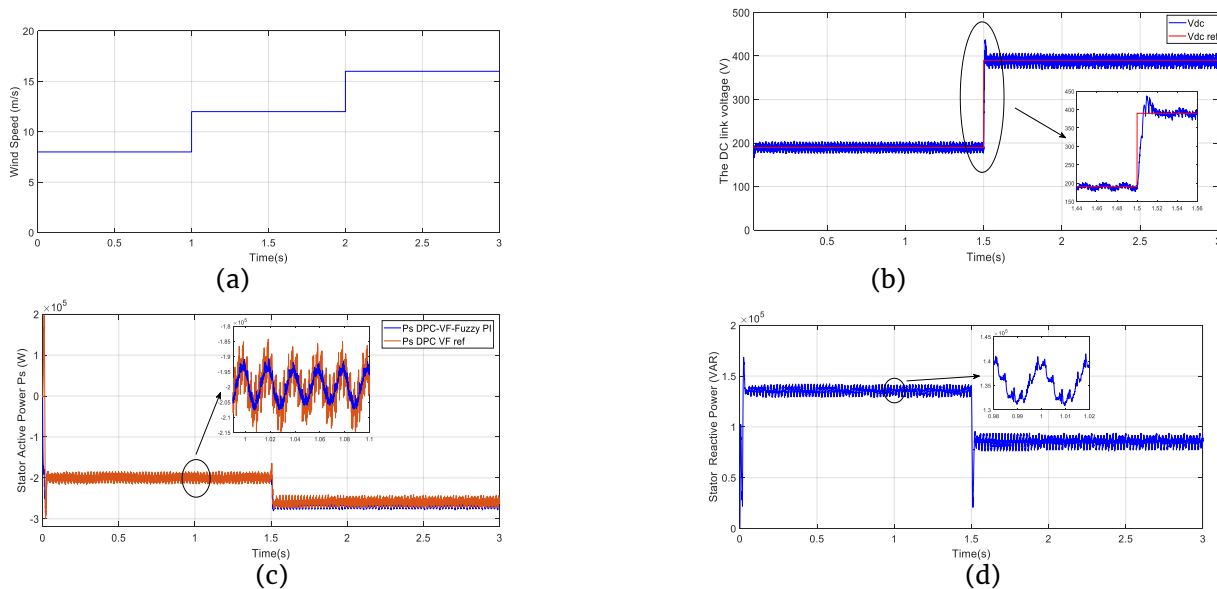
### 5. Results and Discussion

We have tested the robust controller for power with virtual flux estimation controlled doubly fed induction generator drive.

The comparison between the Powers by flux estimation and the real one in Figure 10. (a) reveals that the observation is satisfactory even if there is a difference between these two Powers at the time of the

transitory modes such as powers or Dc voltage rectifier change.

The simulation results confirm the efficiency of the DPC-F-PI-Virtual flux Estimation compared with the IFOC F-PI; these results show that the direct power control with the proposed controller can track the reference command accurately and quickly. Therefore, it able to react positively with an ameliorate DC voltage rectifier.



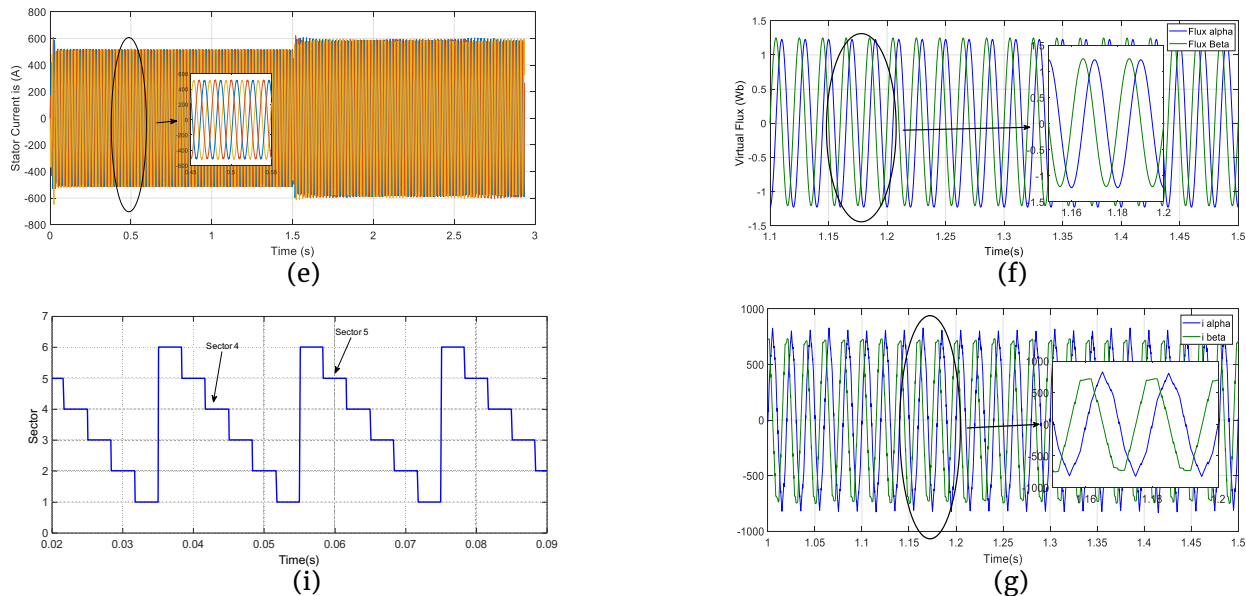


**Figure 9.** Simulation results of the DPC-Fuzzy PI Virtual flux estimation ,(a) Step Change Wind Speed ,(b)the Dc link Voltage,(c) Step Change Stator Active Power (W),(d) Step Change Stator Reactive Power (VAR),(e) Current Stator (A),(f) Virtual flux.(i) 6 sector of 'VF-DPC' estimated ,(g) Stator current  $i_{\alpha}$  , $i_{\beta}$  .

The figure 9 (a) shows the applied step change of wind profile for the studied system, and it could ensure various operation conditions. The wind speed steps from 8 m/s to 11.8 m/s at instant 2 s, and from 11.8 m/s to 16.1 m/s at instant 4 s .

The figure 9 (b) presents the waveform of the DC link voltage. The DC link voltage reference is set to 200 V and 400 V, the measured voltage perfectly follows the reference signal with the exception at 3s small variation of DC-Link voltage due to the passage of 200v to 400v.

The figure 9 (c) shows that our system presents a satisfactory dynamics and an almost zero static error, for the active power one observes a dynamics which reacts quickly and with a weak overshoot. The coupling between the two powers is very weak and hardly noticeable.

The figure 9 (g) presents virtual flux angle estimated using 'Fuzzy-PI' Controller. It can be seen that the phase angle waveform of virtual flux is smooth and stable, then the estimated 'VF' can be used to detect the sector used in control of direct power control.

### 5.1. Robustness test

The robustness of the commands is an important point, especially for systems comprising several

interacting entities or gggf systems with strong parameter variation. These results show the robustness of the proposed new intelligent power adjustment compared with IFOC strategy. On the other hand, it can be observed from Figure 10 which represented the active and reactive powers, by the DPC-Fuzzy PI Virtual flux estimation the system can reach the set point with a large rise time and more steady state error as compared to the conventional IFOC controller. From the results, it is clear that, DPC-Fuzzy PI Virtual flux estimation is more effective than IFOC controllers (shorter settling time and small steady-state error).The control of the active power for the wind generator is perfectly carried out at a unit power factor  $\cos(\phi) = 1$  like as IFOC strategy .



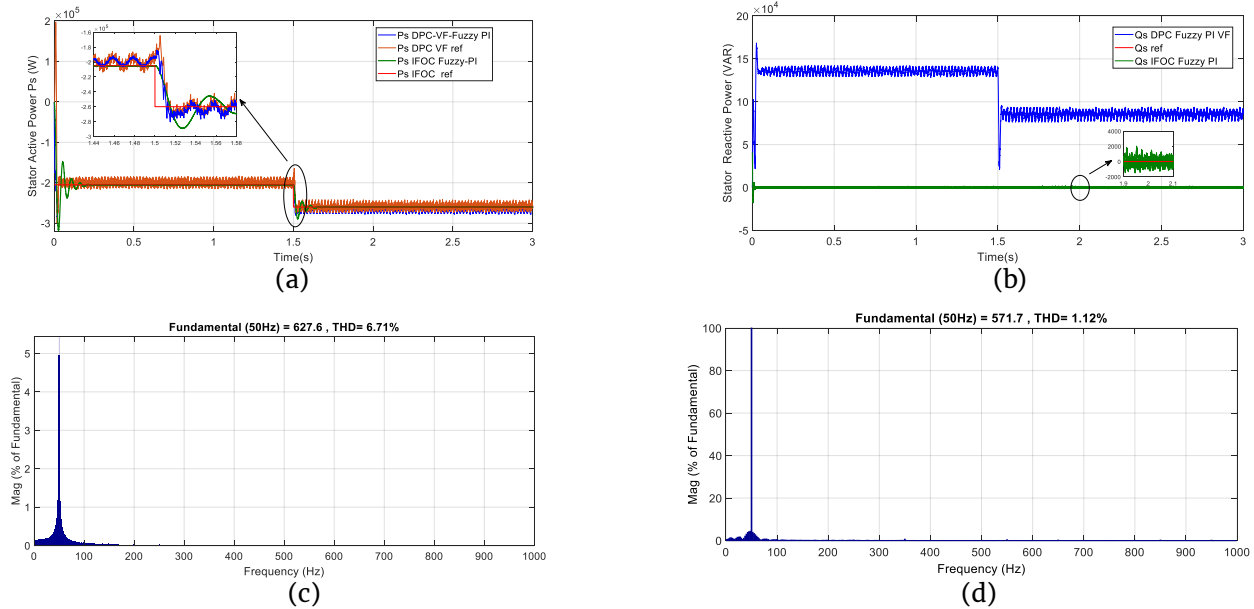


**Figure 10.** Simulation results of the DPC-Fuzzy PI Virtual flux estimation and IFOC Strategy, (a) Stator Active Power (W), (b) Stator Reactive Power (VAR), (c) FFT and THD of IFOC, (d) FFT and THD of DPC Fuzzy PI VF estimation.

### 6. Comparison to the state-of-the-art

Finally, Table 3 summarizes the principal differences between the IFOC strategy and the new Table 3. Comparison of IFOC and DPC-Fuzzy PI-VF.

Intelligent Power Adjustment (DPC-Fuzzy PI-VF).

Control strategy	IFOC [13-15]	DPC-Fuzzy PI-VF
power controllers	Fuzzy-PI controller	Fuzzy-PI and hysteresis band controller
THD	6.71%	1.12%
Fundamental (f=50Hz)	F=627.6	F=571.7
Transitory response	Medium	High
response time	Medium	Fast
System stability (Ps)	High	Good
System stability (Qs) Cos (φ) =1	High	Low
Robustness	Good	Medium
Block diagram complexity	Low	High
virtual flux estimation	not required	required
PWM	required	not required
switching table	not required	required
dq transformation	d-q reference	α-β reference
control structure	High	Medium
implementation	Complex	Simple

### 7. Conclusion

Using IFOC controller, it is very difficult and complex to design a high doubly fed induction generator drive system, and the Fuzzy-PI Controller is very complex with respect to the software and requires an extensive calculation that puts extra load on the processor.

In this paper we presented the states variations in an objective of ameliorate the power adjustment by a DPC –Fuzzy PI-Virtual flux estimation can be used for

parameter estimation as well as state estimation is less sensitive to the system parameters variation and this proves its robustness. A comparison between IFOC and DPC Fuzzy-PI-VF reveals the effectiveness of the first one, and argues that the F-PI-VF estimation has a good performance and is the least involved in terms of design, and DC link voltage and sector detection with precision and more System stability (Active Power Ps).

Future work is oriented at experimental validation.



## References

- [1] H. Jenkal, B. Bossoufi, A. Boulezhar, A. Lilane & S. Hariss, (2020). Vector control of a Doubly Fed Induction Generator wind turbine, *Materials Today : Proceedings*. doi :10.1016/j.matpr.2020.04.360
- [2] H. Benbouhenni, Z. Boudjema, A. Belaidi, (2020). DPC Based on ANFIS Super-Twisting Sliding Mode Algorithm of a Doubly-Fed Induction Generator for Wind Energy System, *Journal Européen des Systèmes Automatisés*, Vol. 53, No. 1, February, 2020, pp.69-80, <https://doi.org/10.18280/jesa.530109>
- [3] B. Yu, M. Dong, M. Ren, Simulation Research on Vector Control Strategy with Feedforward Compensation of Doubly-fed Induction Generator, 2020 IEEE International Conference on Advances in Electrical Engineering and Computer Applications (AEECA), 2020, Dalian, China, 25-27 Aug. 2020, pp 582-586, 10.1109/AEECA49918.2020.9213666
- [4] Y. Zhang, T. Jiang, & J. Jian, (2020). Model-Free Predictive Current Control of a DFIG Using an Ultra-Local Model for Grid Synchronization and Power Regulation. *IEEE Transactions on Energy Conversion*, doi:10.1109/tec.2020.3004567
- [5] S. K. Lagudu, D. Venkata Naga Nagaanth, & S. Madichetty, (2020). Independent Control of Active and Reactive Power for Grid Connected DFIG using Reference Power Based Improved Field-oriented Control Scheme. *International Journal of Ambient Energy*, p:1-18. doi:10.1080/01430750.2020.1818123
- [6] B. Amel, Z. Soraya, C. Abdelkader, Intelligent control of flywheel energy storage system associated with the wind generator for uninterrupted power supply, *International Journal of Power Electronics and Drive System (IJPEDS)*, Vol. 11, No. 4, December 2020, pp. 2062-2072, DOI:10.11591/ijpeds.v11.i4.pp:2062-2072.
- [7] R. Nair, & N. Gopalaratnam, (2020). Stator Flux Based Model Reference Adaptive Observers for Sensorless Vector Control and Direct Voltage Control of Doubly-Fed Induction Generator. *IEEE Transactions on Industry Applications*, pp: 3776 - 3789, 2020, doi:10.1109/tia.2020.2988426 .
- [8] S. Massoum, A. Meroufel, A. Massoum, W. Patrice, DTC based on SVM for induction motor sensorless drive with fuzzy sliding mode speed controller, *International Journal of Electrical and Computer Engineering (IJECE)* Vol. 11, No. 1, February 2021, pp. 171-181 ISSN: 2088-8708, DOI: 10.11591/ijece.v11i1.pp171-181.
- [9] Z. Boulghasoul, Z. Kandoussi, A. Elbacha, & A. Tajer, Fuzzy Improvement on Luenberger Observer Based Induction Motor Parameters Estimation for High Performances Sensorless Drive, *Journal of Electrical Engineering & Technology*, 2020, doi:10.1007/s42835-020-00495-6.
- [10] S. Gao, H. Zhao, Y. Gui, D. Zhou, & F. Blaabjerg, (2020). An Improved Direct Power Control for Doubly Fed Induction Generator. *IEEE Transactions on Power Electronics*, pp: 4672 - 4685. doi:10.1109/tpel.2020.3024620 .
- [11] B. BOSSOUFI, H. A. Aroussi, & M. Boderbala, (2020). Direct Power Control of Wind Power Systems based on DFIG-Generator (WECS). 2020 12th International Conference on Electronics, Computers and Artificial Intelligence (ECAI) 25-27 June. 2020, Bucharest, Romania, doi:10.1109/ecai50035.2020.9223136 .
- [12] X. Yan, M. Cheng, L. Xu, Y. Zeng, Dual-Objective Control Using an SMC-Based CW Current Controller for Cascaded Brushless Doubly Fed Induction Generator, *IEEE Transactions on Industry Applications* ( Volume: 56, Issue: 6, Nov.-Dec. 2020), pp:7109 - 7120, DOI: 10.1109/TIA.2020.3021624.
- [13] A. Tamaarat, Active and Reactive Power Control for DFIG Using PI, Fuzzy Logic and Self-Tuning PI Fuzzy Controllers, *Advances in Modelling and Analysis C* Vol. 74, No. 2-4, December, 2019, pp. 95-102. DOI: [https://doi.org/10.18280/ama\\_c.742-408](https://doi.org/10.18280/ama_c.742-408).
- [14] S. Mensouf, A. Essadki, I. Minka, T. Nasser, B. B. Idrissi, L. Ben Tarla, Performance of a vector control for DFIG driven by wind turbine: real time simulation using DS1104 controller board, *International Journal of Power Electronics and Drive System (IJPEDS)* Vol. 10, No. 2, June 2019, pp. 1003-1013 ISSN: 2088-8694, DOI: 10.11591/ijpeds.v10.i2.1003-1013.
- [15] B. Boujoudi, E. Kheddioui, N. Machkour, M. Bezza, (2019) A Comparative Study Between PI and Sliding Mode Control for the DFIG of a Wind Turbine. In: Derbel N., Zhu Q. (eds) *Modeling, Identification and Control Methods in Renewable Energy Systems*. Green Energy and Technology. Springer, 25 December 2018, Singapore. [https://doi.org/10.1007/978-981-13-1945-7\\_10](https://doi.org/10.1007/978-981-13-1945-7_10).
- [16] S. Khateri-abri, S. Tohidi, & N. Rostami, (2019). Improved Direct Power Control of DFIG Wind Turbine by using a Fuzzy Logic Controller. 2019 10th International Power Electronics, Drive Systems and Technologies Conference (PEDSTC). doi:10.1109/pedstc.2019.8697581 .
- [17] G. Hicham, H. Abdeldjebar, C. Ahmed, Direct Active and Reactive Power Regulation of DFIG Using Fuzzy Adaptive PI Controller, *INTERNATIONAL JOURNAL OF SYSTEMS APPLICATIONS, ENGINEERING & DEVELOPMENT* Volume 13, 2019, pp:161-165.

- [18] S. Thakera ,V. Nagorib , Analysis of Fuzzification Process in Fuzzy Expert System, International Conference on Computational Intelligence and Data Science (ICCIDS 2018), Procedia Computer Science, Volume 132, 2018, Pages 1308-1316, DOI: <https://doi.org/10.1016/j.procs.2018.05.047>

#### Appendix : PARAMETERS

DFIG parameters	Turbine parameters
$P_n = 1.5 \text{ Mw}$	$R = 40 \text{ m}$
$V_s = 220 \text{ V}$	$J = 256 \text{ kgm}^2$
$F = 50 \text{ Hz}$	$G = 70$
$R_s = 3.82 \text{ m}\Omega$	
$R_r = 2.97 \text{ m}\Omega$	
$L_s = 12.241 \text{ mH}$	
$L_r = 12.177 \text{ H}$	
$M = 12.12 \text{ mH}$	
$J = 256 \text{ kg. m}^2$	
$f = 0 \text{ N. m/s}$	
$P = 2$	

